

## Response Letter

We are grateful to the editor and associate editor for their constructive and valuable comments and greatly appreciate their hard work and careful reading of our manuscript. Here we provide point-by-point responses to the seven comments/suggestions raised by the associate editor. The original comments are italicized and shown in blue below. The line numbers in the comments refer to those in the original manuscript, while the line numbers denoted as "new line" refer to those in the revised manuscript. Revised sentences in the response below are indicated in red. In addition to the revisions directly related to the comments, we have also made several minor refinements, as summarized in the "Additional Amendments" section at the end of this letter.

### **Reply to Associate Editor:**

*I have gone through the reviewers' comments and the authors' responses. The authors have made a number of improvements to the manuscript in response to reviewer comments and I believe they have addressed the major concerns. I have a few additional minor comments. The methodology is much clearer now and I think the authors have done an excellent job of explaining themselves, but I still think some comparison of  $k_{sn}$  values from chi-z slopes vs the S-A analysis would be useful (the authors have already collected all the data they need for this).*

Thank you very much for evaluating our revised manuscript. We have improved the manuscript in accordance with your constructive, helpful comments and suggestions as follows.

### **Line 40 and elsewhere:**

*The symbol  $Q$  is almost always used for water discharge so I suggest using the standard notation of  $Q_s$  for sediment flux, especially since in equation (2)  $A$  is serving as a proxy for water discharge.*

Thank you for your comment. We have changed  $Q$  to  $Q_s$  throughout the manuscript, including line 40 and Eq. (2).

### **Line 64:**

*Use a different reference for this, that is not what the Lague paper is about. Cite the original Lal 1991 paper.*

Thank you for your comment. We have changed the citation to '(Lal, 1991)' and added the reference as follows:

Lal, D.: Cosmic ray labeling of erosion surfaces: in situ nuclide production rates and erosion models, *Earth Planet. Sci. Lett.*, 104, 424–439, [https://doi.org/10.1016/0012-821X\(91\)90220-C](https://doi.org/10.1016/0012-821X(91)90220-C), 1991.

### **Figure 1:**

*The inset map showing the region could be clearer: on the scale this is shown it isn't clear what island the site is on*

Thank you for your comment. To improve the clarity of the inset map, we have replaced the small regional map in the upper right of Fig. 1a (formerly showing northeastern Japan only) with a map of the entire Japanese archipelago, so that the location of the study area can be more easily recognized.

[Revision]

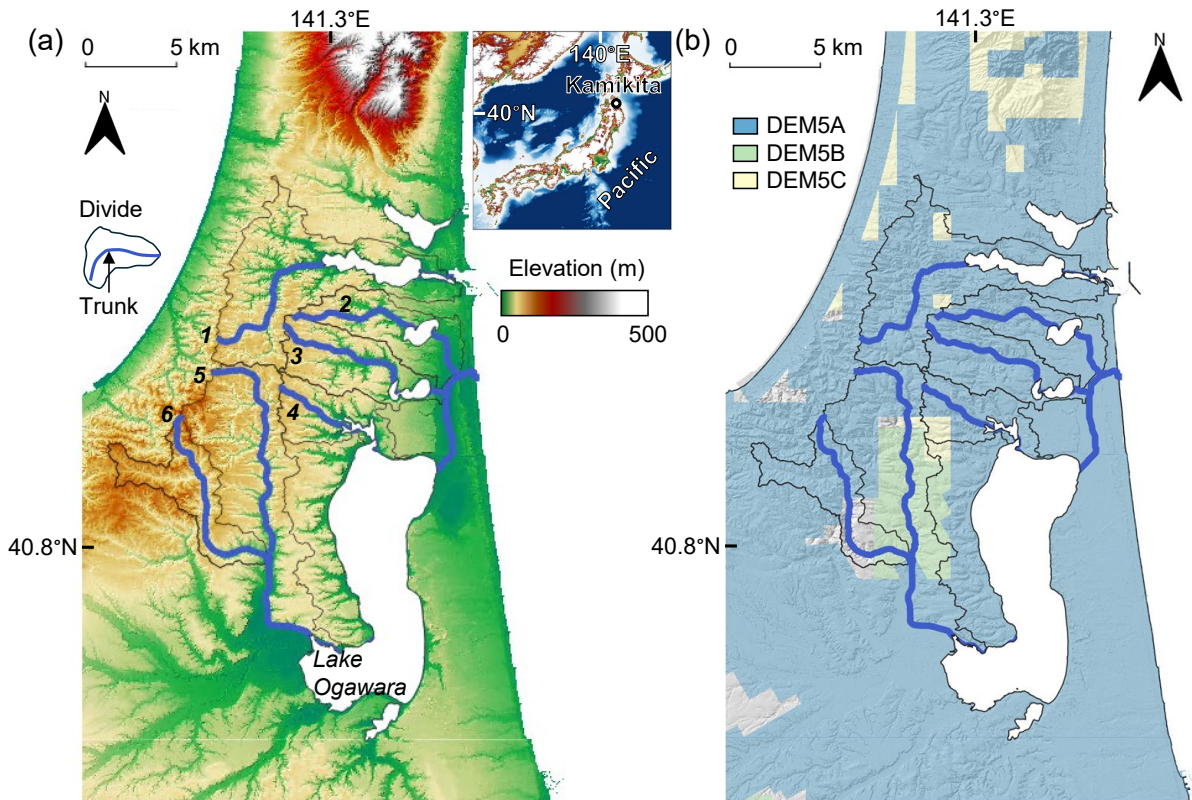


Figure 1: (a) Topography and (b) provided area of 5 m DEM by Geospatial Information Authority of Japan. For area where 5 m DEM is not provided, 10 m DEM was used.

**Line 104:**

*“The valleys are deep...”*

Thank you for your comment. We have changed “The valley is deep” to “The valleys are deep”.

**Line 119:**

*This isn't the stream power law, it is “Flint's law” (which was actually first published by Morisawa in the 60s). It is important not to mix these two things up. The stream power law is an incision rule that predicts, at steady state, the channel slope will be proportional to area with a power of  $m/n$ . Equation 2 is a geometric description of the power law scaling between slope and area generally seen in landscapes and not dependent on any incision law. Parameters from the SPIM can be extracted from equation 2 if certain assumptions hold, but it is not, in itself the stream power law. It is important to state that you are using equation 2 to extract information about the stream power parameters rather than measuring stream power incision directly.*

We appreciate the associate editor's important comment. To address this issue, we have revised the description of Eq. (3) from 'stream power law' to 'Flint's law', and clarified that Eq. (3) describes an empirical slope-area scaling relationship from which stream power incision parameters can be inferred under certain assumptions as follows:

[Original (line 117–122)]

As previous research has shown (e.g., Whipple and Tucker, 2002; Whipple, 2004), most bedrock channels are mixed bedrock-alluvial channels partially covered by alluvium. In this case, the river profile consists of colluvial, bedrock, and alluvial sections (Fig. 3a). In the bedrock section where the DL model holds, Eq. (1) can be rewritten as the stream power law (Hack, 1957; Flint, 1974):

$$S = k_s A^{-\theta}, \quad (3)$$

where  $k_s = (E/K)^{1/n} [L^{2\theta}]$  is the steepness index. This means that in the DL model,...

[Revised (new line 117–126)]

As previous research has shown (e.g., Whipple and Tucker, 2002; Whipple, 2004), most bedrock channels are mixed bedrock-alluvial channels partially covered by alluvium. In this case, the river profile consists of colluvial, bedrock, and alluvial sections (Fig. 3a). **Empirical evidence suggests that many river profiles across different geological settings follow a power-law relationship between  $S$  and  $A$ , known as Flint's law (Hack, 1957; Morisawa, 1962; Flint, 1974):**

$$S = k_s A^{-\theta}, \quad (3)$$

where  $k_s [L^{2\theta}]$  is the steepness index. **The detachment-limited stream power incision model (Eq. (1)) also predicts a similar slope-area scaling. Under the assumptions that  $K$  is constant (e.g., spatially uniform lithology and climate) and  $E$  has been measured (e.g., Hilley et al., 2019), the parameters in Eq. (1) can be inferred from  $k_s (= (E/K)^{(1/n)})$  and  $\theta (= m/n)$  estimated using Eq. (3), without measuring stream power directly.**

**Eq. (3) implies that in detachment-limited reaches,...**

We have also added the following reference:

**Morisawa, M. E.: Quantitative geomorphology of some watersheds in the Appalachian Plateau, Geol. Soc. Am. Bull., 73, 1025–1046, [https://doi.org/10.1130/0016-7606\(1962\)73\[1025:QGOSWI\]2.0.CO;2](https://doi.org/10.1130/0016-7606(1962)73[1025:QGOSWI]2.0.CO;2), 1962.**

### **Line 165:**

*You have calculated  $\chi$ , and  $k_s$  is the gradient of the channel in  $\chi$ -z space, so why not use that (which is less noisy) rather than regression of the  $S$ - $A$  data? I would just report the  $k_{sn}$  measured using the slopes against the  $k_{sn}$  measured using the  $\chi$ -z data.*

We appreciate the associate editor’s insightful comment. We agree that  $k_{sn\_χ}$  ( $k_{sn}$  measured using  $χ$  plot) has lower sensitivity to noise. However, our primary objective includes investigation of transient steepening and lithological signals associated with slope-break knickpoints, which may be partially smoothed in  $k_{sn\_χ}$ . For this reason, we primarily used slope-area-derived  $k_{sn}$ .

To address this comment, we have added an explanation in the Methods section clarifying the differences between  $k_{sn}$  derived from slope-area approach and  $k_{sn\_χ}$ , together with the rationale for primarily using slope-area-derived  $k_{sn}$  in this study. To evaluate the robustness of the results, we additionally calculated channel-averaged  $k_{sn\_χ}$  and compared it with channel-averaged local  $k_{sn}$  derived from the slope-area approach. The revised manuscript now reports that both metrics show very strong correlations ( $R^2 = 0.98–0.99$ ), consistent with previous studies. Although  $k_{sn\_χ}$  yields slightly smaller estimated  $n$  values because of its smoother character, the main conclusions and inter-river trends remain unchanged. These additions have been incorporated into the Discussion section, and the comparison figures are provided in the Supplementary Material as follows:

- Equation (5)

$$z(x) = z(x_b) + \left(\frac{E}{KA_0^m}\right)^{1/n} \chi = z(x_b) + \left(\frac{k_s}{A_0^\theta}\right) \chi, \quad (5)$$

- New line 173–181

[Addition]

As shown in Eq. (3) and (5), local  $k_{sn}$  values and their channel-averaged values can be calculated either from (1) the slope-area approach (e.g., Wobus et al., 2006; Scherler et al., 2014) or (2) the slope of  $χ$  plots (hereafter  $k_{sn\_χ}$ : e.g., Perron and Royden, 2013; Gailleton, 2019). The slope-area approach preserves local signals associated with knickpoints, whereas  $k_{sn\_χ}$  is comparatively smoother and less sensitive to noise (Gailleton, 2019). Previous studies have compared these two approaches (e.g., Scherler et al., 2014; Neely et al., 2017) and demonstrated that the choice of method should depend on the context and objective of a study. In this study, we primarily used local  $k_{sn}$  ( $= SA^{\theta_{ref}}$ ) and its channel-averaged values derived from the slope-area approach (e.g., Takahashi, 2022). This is because our objectives include investigation of the transient steepening and lithological signals associated with slope-break knickpoints, which may be partially smoothed in  $k_{sn\_χ}$  despite its lower sensitivity to noise. For channel-averaged  $k_{sn}$ ,  $k_{sn\_χ}$  was additionally calculated to evaluate the robustness of the results.

- New line 192–193

[Addition]

Because  $χ$  profiles were segmented into channel reaches of unequal length, channel-averaged  $k_{sn\_χ}$  was calculated as the stream-length-weighted mean of segment slopes to avoid overrepresentation of short reaches.

- New line 329–336

[Addition]

To evaluate the robustness of our results, we additionally compared the averaged  $E$  and  $k_{sn_\chi}$ . Similar to previous studies (e.g., Scherler et al., 2014; Neely et al., 2017), channel-averaged local  $k_{sn}$  and  $k_{sn_\chi}$  showed strong correlations ( $R^2 = 0.98$ – $0.99$ ; Fig. S9a-c). Compared with channel-averaged local  $k_{sn}$ , the use of  $k_{sn_\chi}$  yielded slightly smaller  $n$  values ( $0.75$ – $0.83$ ; Fig. S9d-f). This result is consistent with Scherler et al. (2014) and likely reflects the comparatively smoother nature of  $k_{sn_\chi}$ , which reduces the influence of localized transient steepening associated with slope-break knickpoints. Nevertheless, the overall trends remained unchanged regardless of the choice of  $k_{sn}$ : (1) the nonlinear relationship observed for local  $k_{sn}$  ( $n > 1$ ) weakened toward  $n \sim 1$  when channel-averaged  $k_{sn}$  was used, and (2) excluding river No.1 improved the correlation among tributaries within the Takase River basin.

- New line 379–381

[Addition]

Note that the estimated  $K$  value using  $k_{sn_\chi}$  remains within the same order of magnitude as that estimated using channel-averaged local  $k_{sn}$ , differing by less than a factor of two (Fig. S9d-f).

**S4: Comparison of  $k_{sn}$  and  $k_{sn\_X}$**

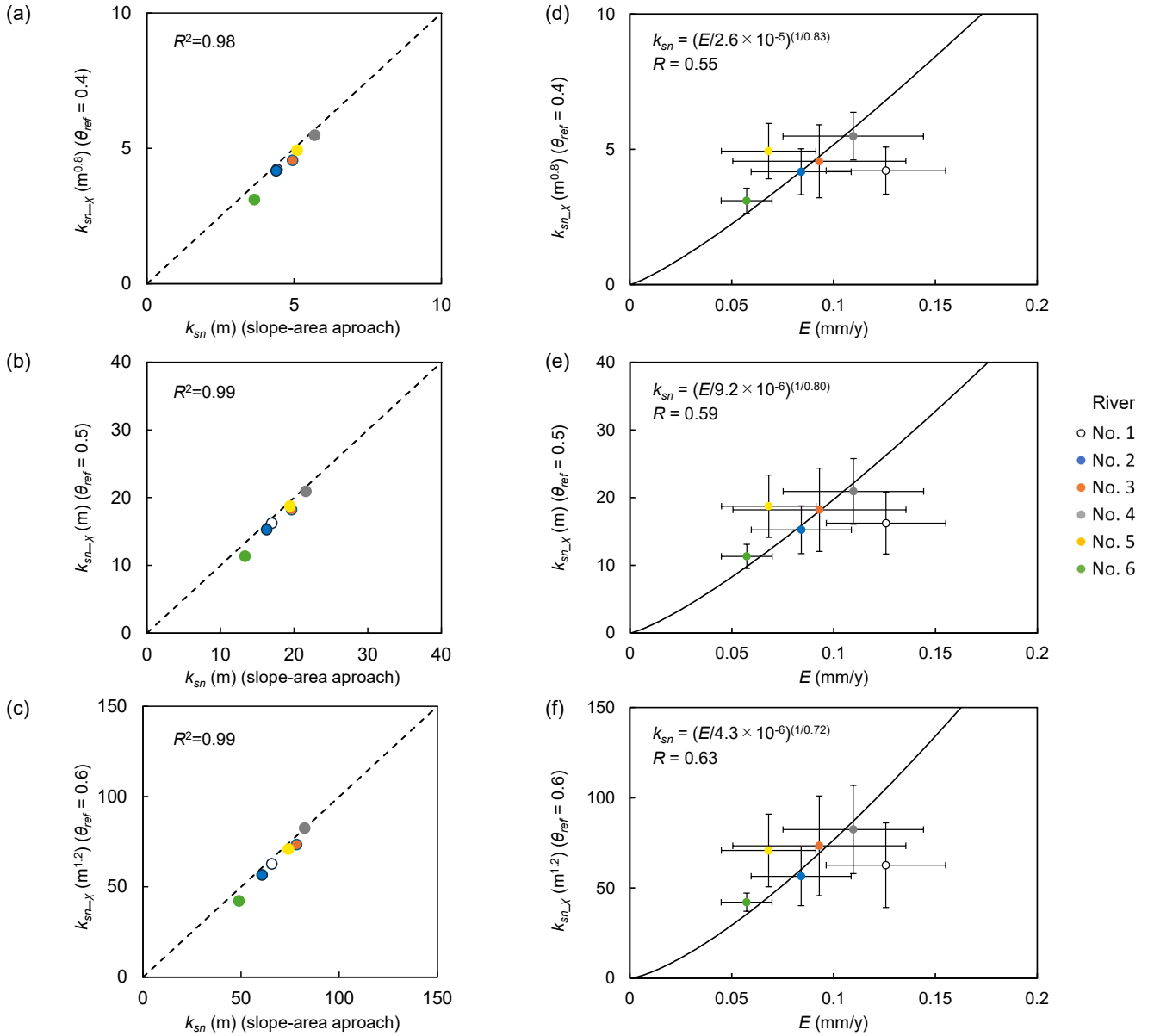


**Figure S9: (a-c) Comparison of  $k_{sn}$  and  $k_{sn\_X}$  and (d-f) channel-averaged river incision rate versus  $k_{sn\_X}$  within the detachment-limited reaches for  $\theta_{ref} = 0.4, 0.5,$  and  $0.6$ . Error bars denote  $\pm 1\sigma$ . The uncertainty  $\sigma$  for  $k_{sn\_X}$  was calculated as  $\sqrt{\sigma_{fit}^2 + \sigma_{between}^2}$ , where  $\sigma_{fit}^2 = \sum_i (w_i \sigma_i)^2 / (\sum_i w_i)^2$  ( $w_i$ : the weight for stream length for segment  $i$ ,  $\sigma_i$ : the standard deviation for the slope of the  $\chi$  plot regression line for segment  $i$ ) and  $\sigma_{between}^2 = \sum_i w_i (k_{sn\_X}^i - k_{sn\_X})^2 / \sum_i w_i$  ( $k_{sn\_X}^i$ :  $k_{sn\_X}$  for segment  $i$ ). Note that  $\sigma_{fit}$  was several orders of magnitude smaller than  $\sigma_{between}$ .**

We have added the following reference:

Neely, A. B., Bookhagen, B., and Burbank, D.W.: An automated knickzone selection algorithm (KZ-Picker) to analyze transient landscapes: Calibration and validation, *J. Geophys. Res. Earth Surf.*, 122, 1236–1261, <https://doi.org/10.1002/2017JF004250>, 2017.

Scherler, D., Bookhagen, B., and Strecker, M. R.: Tectonic control on 10 Be-derived erosion rates in the Garhwal Himalaya, India, *J. Geophys. Res.-Earth*, 119, 83–105, <https://doi.org/10.1002/2013JF002955>, 2014.

Takahashi, N. O., Shyu, J. B. H., Chen, C., and Toda, S: Long-term uplift pattern recorded by rivers across contrasting lithology: Insights into earthquake recurrence in the epicentral area of the 2016 Kumamoto earthquake, Japan, *Geomorphology*, 419, <https://doi.org/10.1016/j.geomorph.2022.108492>, 2022.

**Line 300:**

*Gasparini and Brandon (2011, JGR-ES) specifically looked at how these factors can be expressed as nonlinearity in the SPIM so that should be cited here.*

Thank you for the comment. We have added the reference and revised the sentence as follows:

[Original (line 318–320)]

Such physical factors include shear stress thresholds, abrasion, plucking, and channel-width effects (Whipple et al., 2000), as well as tool and cover effects (Yamanashi and Naruse, 2025).

[Revision (new line 345–347)]

Such physical factors include shear stress thresholds, plucking, channel-width effects, **and sediment-flux-dependent incision processes such as abrasion, tool effects**, and cover effects (Whipple et al., 2000; **Gasparini and Brandon, 2011**; Yamanashi and Naruse, 2025).

We have added the following reference:

Gasparini, N. M. and Brandon, M. T.: A generalized power law approximation for fluvial incision of bedrock channels, *J. Geophys. Res.*, 116, <https://doi.org/10.1029/2009jf001655>, 2011.

**Additional Amendments:**

In addition to the above comments, the following amendments have been made.

[New line 197–200]

We noticed that the thresholds for knickpoint extraction were not described in the manuscript. We have added the information to the Methods section as follows:

To remove minor knickpoints, we applied thresholds of  $Z_{jump} = 5.0$  m and  $S_{ratio} = 0.2$ . These values are broadly consistent with those used in previous studies: Neely et al. (2017) applied a minimum knickzone height of 5 m for 10 m DEM, and Gailleton et al. (2019) used a threshold of  $|Δk_{sn}|$  (the difference in slope of regression lines) = 0.8 for  $k_{sn}$  values ranging from 0.5 to 5.0.

#### [Figure 7]

We noticed that the unit of  $k_{sn}$  on the vertical axis of Fig. 7 was incorrectly labeled as m throughout. We have corrected it to the appropriate unit corresponding to  $L^{2θ}$  (i.e.,  $m^{0.8}$ , m,  $m^{1.2}$  for  $θ = 0.4, 0.5, 0.6$ , respectively).

#### [Figure 8]

We noticed that the horizontal axis label of Figure 8 contained an error: the unit of  $E$  used in the  $K$  estimation was mm/yr, which caused the axis values to be offset by  $-3$  in  $\log_{10}$  space. The axis has been corrected accordingly. All  $K$  values reported in the text and other figures are unaffected.